



Synthesis of fluorinated alkoxyamines and alkoxyamine-initiated nitroxide-mediated precipitation polymerizations of styrene in supercritical carbon dioxide

Title	Synthesis of fluorinated alkoxyamines and alkoxyamine-initiated nitroxide-mediated precipitation polymerizations of styrene in supercritical carbon dioxide
Author(s)	Magee, Christopher;Earla, Aruna;Petraitis, Jennifer;Higa, Chad;Braslau, Rebecca;Zetterlund, Per B.;Aldabbagh, Fawaz
Publication Date	2014-06-20
Publisher	Royal Society of Chemistry
Repository DOI	10.1039/C4PY00757C

Synthesis of fluorinated alkoxyamines and alkoxyamine-initiated nitroxide-mediated precipitation polymerizations of styrene in supercritical carbon dioxide†

Christopher Magee,^a Aruna Earla,^b Jennifer Petraitis,^b Chad Higa,^b Rebecca Braslau,^{*b} Per B. Zetterlund^{*c} and Fawaz Aldabbagh^{*a}

TIPNO (2,2,5-trimethyl-4-phenyl-3-azahexane-3-nitroxide)-alkoxyamine was found to give reasonably controlled/living nitroxide-mediated (NMP) precipitation polymerizations of styrene in supercritical carbon dioxide (scCO₂). In contrast under the same conditions, the analogous SG1 (*N-tert-butyl-N*-(1-diethylphosphono-2,2-dimethylpropyl) nitroxide)-alkoxyamine gave higher rates of polymerization and inferior controlled/living character. The circumvention of the requirement for excess free [nitroxide]₀ allowed the study of nitroxide partitioning effects in scCO₂ for three newly synthesized fluorinated alkoxyamines. Two alkoxyamines dissociated into scCO₂-philic fluorinated TIPNO-nitroxide derivatives, while another contains a similar sized fluorinated “foot”. Despite the increase steric bulk about the N-O bond for the novel fluorinated alkoxyamines, all polymerizations proceeded at a similar rate and level of control to the TIPNO system in solution (toluene). PREDICI simulations for the styrene/TIPNO system are used to support extensive partitioning effects observed in scCO₂ for the fluorinated alkoxyamines.

Introduction

Supercritical carbon dioxide (scCO₂) is a benign solvent used to circumvent the requirement for environmentally damaging volatile organic solvents.¹⁻³ Advantages include a readily accessible critical point (31 °C and 7.4 MPa),⁴ variable solubility by subtle changes in pressure and temperature,⁵ and the lack of chain transfer to solvent in radical polymerizations.^{6, 7} It is particularly well-suited for heterogeneous radical polymerizations, since reagents such as the monomer, initiator and controlling agent are generally soluble in scCO₂, but the resultant polymer is insoluble and precipitates.^{2, 3} If the precipitation system is carried out in the presence of a colloidal stabilizer to prevent coagulation of particles, then dispersion polymerization results giving polymer of narrow particle size

distributions and well-defined particles ($d \approx 100$ nm to 15 μ m).¹⁻³ The monomer is not always soluble in the reaction medium, such as in the controlled/living nitroxide-mediated radical polymerization (NMP) of *N*-isopropylacrylamide (NIPAM) in scCO₂, where an inverse suspension system is generated.^{8, 9} In recent years, there has been a proliferation in the numbers of reported controlled/living precipitation and dispersion polymerizations in scCO₂ with NMP,⁹⁻²¹ atom transfer radical polymerization (ATRP),²²⁻²⁹ reversible addition-fragmentation chain transfer (RAFT)^{3, 30-39} and iodine transfer polymerization (ITP).^{40, 41} The slow build up in molecular weight (MW) in a controlled/living system by virtue of the equilibrium between active propagating radicals and dormant polymer chains allows measurement of the critical degree of polymerization (J_{crit}) before polymer chains precipitate from solution or the continuous phase (containing monomer and scCO₂). After J_{crit} , the polymerization continues in the monomer-rich particle phase. For controlled/living precipitation/dispersion polymerizations, J_{crit} can be predicted as a function of targeted molecular weight and initial monomer loading.¹⁹ In contrast, in a non-living conventional radical polymerization, no single J_{crit} value can be applied due to polymer chains instantaneously reaching high MW and continually precipitating. NMP of styrene in scCO₂ at high monomer loadings (70% w/v) is superior in terms of control over the molecular weight distribution (MWD) for the SG1 (*N-tert-butyl-N*-(1-diethylphosphono-2,2-dimethylpropyl) nitroxide) / AIBN (2,2'-

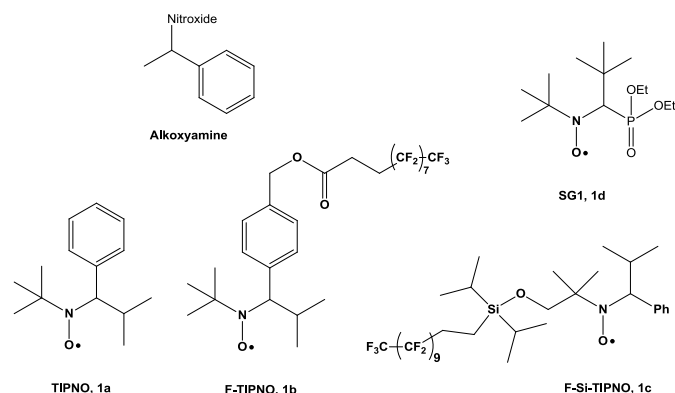
^aSchool of Chemistry, National University of Ireland Galway, University Road, Galway, Ireland. E-mail: fawaz.aldabbagh@nuigalway.ie; Tel: +353 91 493120

^bDepartment of Chemistry and Biochemistry, University of California, 1156 High Street, Santa Cruz, CA 95064, United States. Email: rbraslau@ucsc.edu; Tel: +1 831 459 3087

^cCentre for Advanced Macromolecular Design (CAMD), School of Chemical Engineering, The University of New South Wales, Sydney, NSW 2052, Australia. E-mail: p.zetterlund@unsw.edu.au; Tel: +61 2 9385 6250.

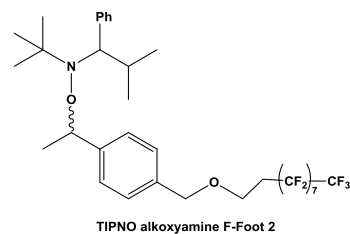
† Electronic supplementary information (ESI) available: NMRs of alkoxyamines, molecular weight distributions for polymerizations and additional kinetic data for the effect of free TIPNO on NMP in scCO₂.

azoisobutyronitrile) precipitation system in comparison to solution (toluene) polymerization carried out under analogous conditions.¹⁷ The effect of nitroxide partitioning upon control was found to be extenuated at low styrene loadings,¹⁵ where the system becomes heterogeneous sooner due to a lower J_{crit} . In that work, the bimolecular nitroxide/AIBN system was used,^{13, 15-17} leading to uncertainty in initiator efficiencies due to unknown amounts of alkoxyamine generated in situ. Control was facilitated by using excess amounts of nitroxide relative to initiating AIBN-derived radicals in order to negate the loss of nitroxide from the locus of polymerization via partitioning, as well as side-reactions occurring at the initial stages of alkoxyamine formation and during polymerization. In the present article controlled/living precipitation NMP in $scCO_2$ has for the first time been achieved in the absence of excess free nitroxide. The effect of partitioning on nitroxide and styryl-initiating fragments (“foot” part of alkoxyamine) is examined by preparing and using three new alkoxyamine initiators. Preparation of the fluorinated nitroxides required incorporation of functional handles in the TIPNO (2,2,5-trimethyl-4-phenyl-3-azahexane-3-nitroxide) nitroxide (either on the phenyl portion, or the *t*-butyl fragment), whereas introduction of a fluorinated-labelled foot was easily accomplished by modification of the popular benzyl chloride alkoxyamine⁴² prepared with regular TIPNO.



Scheme 1 Chemical structures of styryl-alkoxyamine initiators **1a-1d** with the four nitroxide fragments investigated.

Two alkoxyamines dissociate into $scCO_2$ -philic fluorinated TIPNO-nitroxide derivatives (F-TIPNO **1b** and F-Si-TIPNO **1c**, Scheme 1), while another contains a similar sized fluorinated “foot” (TIPNO alkoxyamine F-foot **2**, Scheme 2), which will remain attached to the growing polymer chain. The performance of these fluorinated alkoxyamines in polymerizations of styrene in $scCO_2$ is compared with analogous polymerizations in solution, as well as, TIPNO and SG1-alkoxyamine **1a** and **1d** analogues.



Scheme 2 Chemical structure of TIPNO-alkoxyamine **2** containing fluorinated styryl “foot”

Experimental

Materials

Styrene monomer (Aldrich, >99%) was distilled under reduced pressure prior to use. Reagent grade toluene (Aldrich, >99.7%), THF (Aldrich >99%), methanol, ethanol, CO_2 (BOC gases, 99.8%), trimethylacetaldehyde (Aldrich, 96%), diethyl phosphite (Aldrich, 98%), *tert*-butyl amine (Aldrich, 98%), ethylenediamine (Aldrich, 99%), salicylaldehyde (Aldrich, 98%), manganese (II) acetate tetrahydrate (Aldrich, 99%), sodium chloride (Aldrich, 99%), sodium borohydride (Aldrich, 99%), 4,4,5,5,6,6,7,7,8,8,9,9,10,10,11,11,11-heptadecafluoroundecanoyl chloride (Santa Cruz Biotechnology), triethyl amine (Aldrich), ethylenediamine (Aldrich), $Mn(OAc)_2 \cdot 4H_2O$ (Acros Organics), pyridine (Acros Organics), (3,3,4,4,5,5,6,6,7,7,8,8,9,9,10,10,11,11,12,12,12-henicosafuorododecyl), diisopropyl-silane (Fluorous Technologies Inc.), trifluoromethanesulfonic acid (TCI America), 1*H*, 1*H*, 2*H*, 2*H*-perfluorodecanol (Matrix Scientific), tetrabutylammoniumhydrogen sulfate (TCI America), 2-hydroxybenzaldehyde (EMD), and sodium hydroxide (Fisher Scientific) were used as received. Dichloromethane (Fisher Scientific) was dried over calcium hydride (Fisher Scientific) when anhydrous conditions were required. NMR solvents $CDCl_3$ and C_6F_6 were obtained from Cambridge Isotope Laboratories and used as received. TIPNO⁴³ (2,2,5-trimethyl-4-phenyl-3-azahexane-3-nitroxide) and SG1⁴⁴ (*N*-*tert*-butyl-*N*-(1-diethylphosphono-2,2-dimethylpropyl) nitroxide) were prepared according to the literature. TIPNO alkoxyamine (2,2,5-trimethyl-3-(1-phenylethoxy)-4-phenyl-3-azahexane) and SG1 alkoxyamine (diethyl(1-[*tert*-butyl(1-phenylethoxy)amino]-2,2-dimethylpropyl)phosphonate) were prepared by reaction of the appropriate free nitroxide with styrene using a $Mn(salen)$ catalyst.⁴⁵ The preparations of F-TIPNO **1b**, F-Si-TIPNO **1c** and F-TIPNO-foot **2** alkoxyamines and the $Mn(salen)$ catalyst are described below.

Characterization of alkoxyamines

NMR spectra were recorded at ambient temperature on a Varian 500 MHz spectrometer in $CDCl_3$ as solvent unless otherwise noted. C_6F_6 ($\delta -164.9 \text{ ppm}$) was used as reference for ^{19}F NMR. FTIR spectra were recorded on a Perkin-Elmer spectrometer as a neat film on a KBr cell. High resolution mass spectra (HRMS) were recorded on a benchtop Mariner electrospray ionization time-of-flight (ESITOF) mass spectrometer.

Synthesis of alkoxyamines

Preparation of *N,N'*-ethylenebis(salicylimine) ligand

Ethylenediamine (3.000 g, 49.92 mmol) dissolved in 250 mL of absolute ethanol, and 2-hydroxybenzaldehyde (12.191 g, 99.83 mmol) was added: a yellow precipitate formed. The mixture was heated to reflux for 30 minutes; all of the precipitate dissolved to form a yellow solution. Crystals formed upon cooling to room temperature. Additional cooling in an ice-water bath for 30 minutes followed by filtration resulted in 12.570 g (94% yield) of *N,N'*-ethylenebis(salicylimine) as large yellow flakes.

Preparation of Mn(salen) chloride oxo catalyst

To a 500 mL two-necked flask equipped with a reflux condenser was added *N,N'*-ethylenebis(salicylimine) (12.570 g, 46.849 mmol), Mn(OAc)₂·4H₂O (22.970 g, 93.698 mmol) and 180 mL of methanol. Air was bubbled through the solution while being heated to reflux. After 3 hours, an aqueous solution of LiCl (9.930 g, 234.2 mmol in 70 mL of H₂O) was added to the refluxing solution. Reflux concurrent with air bubbling through the solution was continued for another 2 hours. After cooling to room temperature, the mixture was cooled with an ice water bath for 1 hour. The resulting precipitate was isolated by filtration. Additional crops of crystals were obtained by addition of water to the mother liquors and cooling in an ice bath to give a total of 12.728 g. The first batch of precipitate contains both an orange-brown clay-like material, and darker brown precipitate with a sand-like texture. The orange precipitate was not an effective catalyst for alkoxyamine formation. The later crops gave the darker brown precipitate. This is the active catalyst. The combined dark brown material was recrystallized once from boiling water including a hot filtration to give 7.898 g (45% yield) of black crystals (mp > 260 °C), which are a reliable catalyst for alkoxyamine formation.

Preparation of F-TIPNO 1b

To a solution of TIPNO-OH alkoxyamine⁴⁶ (0.6962 g, 1.961 mmol) and 4,4,5,5,6,6,7,7,8,8,9,9,10,10,11,11,11-heptadecafluoroundecanoyl chloride (1.001 g, 1.961 mmol) in 30 mL of anhydrous dichloromethane was added triethylamine (0.1997 g, 1.961 mmol) at room temperature. The reaction mixture was stirred for 1 hour, then 50 mL of dichloromethane and 50 mL of H₂O were added. The layers were separated; the organic layer was washed two times with 30 mL of brine, dried over MgSO₄, and concentrated *in vacuo*. The resulting crude oil (2.136 g) was purified by silica gel column chromatography using 95:5 hexanes/ethyl acetate as eluent, to give the *title compound 1b* as a colorless oil, 1.445 g, (87% yield) as a 1:1 mixture of diastereomers. TLC: 90:10 hexanes/ethyl acetate, UV, *p*-anisaldehyde, *R*_f: 0.62. ¹H NMR (500 MHz, CDCl₃, both diastereomers): δ 7.54 - 7.15 (m, 18H), 5.18 (s, 2H), 5.11 (s, 2H), 4.95-4.90 (m, 2H), 3.45 (d, *J* = 10.6 Hz, 1H), 3.33 (d, *J* = 10.6 Hz, 1H), 2.73-2.67 (m, 4H), 2.55-2.45 (m, 4H), 2.36-2.31 (m, 1H), 1.64 (d, *J* = 6.6 Hz, 3H), 1.56 (d, *J* = 6.6 Hz, 3H), 1.43-1.35 (m, 1H), 1.32 (d, *J* = 6.4 Hz, 3H), 1.06 (s, 9H), 0.94 (d, *J* =

6.4 Hz, 3H), 0.79 (s, 9H), 0.55 (d, *J* = 6.6 Hz, 3H), 0.22 (d, *J* = 6.6 Hz, 3H) ppm. ¹³C NMR (125 MHz, CDCl₃, DEPT, both diastereomers): δ 171.15, 148.27, 145.76, 142.97, 142.77, 133.34, 133.26, 131.30 (CH), 128.21 (CH), 127.51 (CH), 127.37 (CH), 127.15 (CH), 126.82 (CH), 126.32 (CH), 83.65 (CH), 83.02 (CH), 71.99 (CH), 71.87 (CH), 67.06 (CH₂), 60.58, 60.45, 32.08 (CH), 31.68 (CH), 28.44 (CH₃), 28.26 (CH₃), 26.82 (CH₂), 26.65 (CH₂), 25.67(CH₂), 25.67(CH₂), 24.59 (CH₃), 23.05 (CH₃), 22.09 (CH₃), 21.94 (CH₃), 21.13 (CH₃), 21.01 (CH₃) ppm. ¹⁹F NMR (470 MHz, CDCl₃): δ -82.9 (t, *J* = 9.9 Hz, 4F), -116.9 to -117.0 (m, 4F), -123.7 to -123.9 (m, 4F), -123.8 to -123.9 (m, 4F), -124.0 to -124.1(m, 4F), -124.8 to -124.9 (m, 4F), -125.6 (t, *J* = 14.6 Hz, 6F), -128.2 to -128.3 (m, 4F) ppm. FTIR: 3025 (aromatic C-H stretch), 2969 (benzylic C-H stretch), 1744 (C=O stretch), 1449 and 1365 (N-O stretch), 1428 (aromatic C=C stretch), 1204 (C-O stretch), 815 (*p*-substituted benzene), 699 (mono substituted benzene) cm⁻¹. HRMS: calcd. for C₃₄H₃₆F₁₇NO₃ [M+H]⁺: 830.2486; found 830.2502.

Preparation of F-Si-TIPNO 1c

TIPNO-neopentyl-OH alkoxyamine was synthesized as previously described.⁴⁷ Following the procedure of Crich et al.,⁴⁸ a mixture of di-*isopropyl*-(1*H*,1*H*,2*H*,2*H*-perfluorododecyl)silane (0.3012 g, 0.4549 mmol) and trifluoromethanesulfonic acid (0.6827 g, 0.4549 mmol) was added to a flame-dried round bottom flask and stirred under nitrogen for 48 hours. The reaction mixture was diluted with 1 mL of dichloromethane and a solution of TIPNO-neopentyl-OH-alkoxyamine (0.1032 g, 0.3026 mmol), and pyridine (0.036 mL, 0.455 mmol) in 1 mL of dichloromethane was added at 0 °C. The reaction mixture was stirred at 0 °C for 1 hour, diluted with 15 mL of dichloromethane, washed sequentially with H₂O (10 mL), sat. NH₄Cl solution (10 mL), brine (10 mL), dried over MgSO₄, and concentrated *in vacuo*. The resulting crude oil (0.3503 g) was purified by silica gel column chromatography with 90:10 hexanes/ethyl acetate as eluent to give the *title compound 1c* as a colorless viscous oil 0.1081 g (36% yield) as a 1:1 mixture of diastereomers.

TLC: 90:10 hexanes/ethyl acetate, UV, *p*-anisaldehyde, *R*_f: 0.70. ¹H NMR (500 MHz, CDCl₃, both diastereomers): δ 7.62 - 7.12 (m, 20H), 4.88 (m, 2H), 3.56 (d, *J* = 9.2 Hz, 1H), 3.48 (d, *J* = 10.5 Hz, 1H), 3.40 (d, *J* = 9.2 Hz, 1H), 3.32 (d, *J* = 10.5 Hz, 1H), 3.08 (d, *J* = 9.0 Hz, 1H), 3.00 (d, *J* = 9.0 Hz, 1H), 2.39 - 2.36 (m, 1H), 2.25 - 2.12 (m, 2H), 2.01 - 1.80 (m, 2H), 1.62 (d, *J* = 6.6 Hz, 3H), 1.55 (d, *J* = 6.6 Hz, 3H), 1.53 (s, 3H), 1.41-1.35 (m, 1H), 1.32 (d, *J* = 6.6 Hz, 3H), 1.17 (s, 3H), 1.20 - 0.99 (m, 12H), 0.96 (s, 3H), 0.93 (d, *J* = 6.6 Hz, 3H), 0.88-0.80 (m, 16H), 0.77-0.66 (m, 4H), 0.63 (s, 3H), 0.56 (d, *J* = 6.6 Hz, 3H), 0.23 (d, *J* = 6.6 Hz, 3H) ppm. ¹³C NMR (125 MHz, CDCl₃, DEPT, both diastereomers): δ 145.74, 142.66, 130.80 (CH), 128.39 (CH), 128.22 (CH), 127.68 (CH), 127.51 (CH), 127.01 (CH), 126.68 (CH), 126.62 (CH), 126.51 (CH), 126.14 (CH), 83.78 (CH), 82.93 (CH), 72.28 (CH), 72.18 (CH), 70.05 (CH₂), 69.78 (CH₂), 64.76, 64.62, 31.94 (CH), 31.54 (CH), 25.41 (CH₂), 24.83 (CH₂), 24.10 (CH₃), 23.68 (CH₃), 23.26 (CH₃), 21.91 (CH₃), 21.55 (CH₃), 21.22 (CH₃), 20.40 (CH₃), 17.59 (CH₃), 17.49 (CH₃), 17.41 (CH₃), 12.40 (CH₂), 12.12 (CH₂) ppm. ¹⁹F NMR (470 MHz, CDCl₃, both diastereomers): δ -83.0 (t, *J* = 9.9 Hz, 2F), -83.2 (t, *J* = 9.9 Hz,

2F), -118.6 to -118.9 (m, 2F), -119.1 to -119.2 (m, 2F), -124.0 to -124.1 (m, 10F), -124.1 to -124.3 (m, 10F), -124.9 to -125.0 (m, 2F), -125.1 to -125.2 (m, 2F), -125.4 to -125.6 (m, 2F), -125.8 to -125.9 (m, 2F), -128.4 (t, $J = 13.8$ Hz, 3F), -128.5 (t, $J = 13.8$ Hz, 3F) ppm. FTIR: 3056 (aromatic C-H stretch), 2969 (benzylic C-H stretch), 1453 and 1363 (N-O stretch), 1428 (aromatic C=C stretch), 1211 (Si-O stretch), 1150 (C-O stretch), 815 (*p*-substituted benzene), 699 (mono substituted benzene) cm^{-1} . HRMS: calcd. for $\text{C}_{40}\text{H}_{48}\text{F}_{21}\text{NO}_2\text{Si}$ $[\text{M}+\text{H}]^+$: 1002.3186; found 1002.3162.

Preparation of TIPNO-F-Foot 2

TIPNO-benzyl Cl alkoxyamine was synthesized as previously described.⁴³ Following the procedure of Denifl and co-workers,⁴⁹ a solution of 1*H*, 1*H*, 2*H*, 2*H*-perfluorodecanol (8.715 g, 18.77 mmol) and tetrabutylammonium hydrogen sulfate (TBAH) (1.912 g, 5.633 mmol) in 44 mL of 50% aqueous NaOH and 45 mL of dichloromethane was stirred vigorously for 10 minutes. A solution of TIPNO-benzyl Cl alkoxyamine (1.752 g, 4.694 mmol) in 45 mL of dichloromethane was added and the reaction mixture was heated to 40 °C for 2.5 hours. After cooling to room temperature, the layers were separated, and the aqueous layer was extracted three times with 50 mL of dichloromethane. The organic layers were combined, washed three times with 50 mL of 0.1 M hydrochloric acid, dried over MgSO_4 , and concentrated *in vacuo*. The resulting crude oil (3.527 g) was purified by silica gel column chromatography with 98:2 hexanes/ethyl acetate as eluent to give the *title compound* as pale yellow oil 2.353 g (63% yield) as a 2.7:1 mixture of diastereomers. ¹H NMR (500 MHz, CDCl_3 , both diastereomers): δ 7.55 – 7.09 (m, 18H), 4.93 (m, 2H), 4.55 (s, 2H), 4.51 (s, 2H), 3.75 (m, 4H), 3.43 (d, $J = 10.4$ Hz, 1H), 3.31 (d, $J = 10.4$ Hz, 1H), 2.43–2.38 (m, 4H), 2.36–2.28 (m, 1H), 1.62 (d, $J = 6.6$ Hz, 3H), 1.32 (d, $J = 6.6$ Hz, 3H), 1.30 (d, $J = 6.3$ Hz, 3H), 1.05 (s, 9H), 1.02 – 0.96 (m, 1H), 0.92 (d, $J = 6.3$ Hz, 3H), 0.78 (s, 9H), 0.54 (d, $J = 6.6$ Hz, 3H), 0.21 (d, $J = 6.6$ Hz, 3H) ppm. ¹³C NMR (125 MHz, CDCl_3 , DEPT, both diastereomers): δ 145.67, 144.91, 136.59, 135.95, 131.11 (CH), 131.02 (CH), 127.69 (CH), 127.63 (CH), 127.49 (CH), 127.27 (CH), 126.45 (CH), 126.31 (CH), 83.38 (CH), 82.57 (CH), 73.27 (CH_2), 73.19 (CH_2), 72.24 (CH), 72.19 (CH), 62.10 (CH_2), 61.91 (CH_2), 59.66, 59.63, 32.03 (CH), 31.68 ($\text{CH}_2\text{-CF}_2$), 31.63 ($\text{CH}_2\text{-CF}_2$), 31.63 (CH), 28.36 (CH_3), 28.17 (CH_3), 24.66 (CH_3), 23.15 (CH_3), 22.11 (CH_3), 21.94 (CH_3), 21.11 (CH_3), 20.96 (CH_3) ppm. ¹⁹F NMR (470 MHz, CDCl_3 , both diastereomers): δ -82.9 (t, $J = 10.0$ Hz, 2F), -83.1 (t, $J = 10$ Hz, 2F), -115.5 to -115.7 (m, 2F), -115.7 to -115.8 (m, 2F) -123.8 to -124.00 (m, 4F), -124.1 to -124.0 (m, 8F), -124.8 to -124.9 (m, 4F), 125.8 to -125.9 (m, 4F), -128.3 to -128.4 (m, 6F) ppm. FTIR: 3034 (aromatic C-H stretch), 2943 (benzylic C-H stretch), 1492 and 1365 (N-O stretch), 1466 (aromatic C=C stretch), 1243 (C-O stretch), 1152 (aliphatic C-O stretch), 882 (*p*-substituted benzene), 699 (mono substituted benzene) cm^{-1} . HRMS: calcd. for $\text{C}_{33}\text{H}_{36}\text{F}_{17}\text{NO}_2$ $[\text{M}+\text{H}]^+$: 802.2547; found 802.2307.

Equipment and measurements for polymerizations

All NMP in scCO_2 were conducted in a 25 ml stainless steel Parr reactor with a maximum operating pressure of 40 MPa and 130 °C. The pressure was achieved using a Thar P-50 series high pressure

pump and temperature was monitored by a Thar CN6 controller. M_n and polydispersity (M_w/M_n) were determined using a gel permeation chromatography (GPC) system consisting of a Viscotek DM 400 data manager, a Viscotek VE 3580 refractive-index detector, and two Viscotek Viscogel GMH_{HR}-M columns. Measurements were carried out at 60 °C at a flow rate of 1.0 mL min^{-1} using HPLC-grade DMF containing 0.01 M LiBr as the eluent. The columns were calibrated using twelve polystyrene standards ($M_n = 580\text{-}6,035,000$ g mol^{-1}). M_n is given in g mol^{-1} throughout. The theoretical value of M_n ($M_{n,\text{th}}$) is calculated using equation 1:

$$M_{n,\text{th}} = \frac{\alpha[M]_0 MW_{\text{mon}}}{[\text{Alkoxyamine}]_0} + MW_{\text{Alk}} \quad (1)$$

where α is fractional conversion of monomer, $[M]_0$ is the initial monomer concentration, MW_{mon} and MW_{Alk} are the molecular weights of monomer and alkoxyamine. Reaction mixtures were added to a large excess of methanol to precipitate polystyrene. The polymer was filtered, dissolved in THF and re-precipitated from methanol. The polymer was dried under vacuum at room temperature for 24 hours before conversion was measured by gravimetry.

Solution polymerizations

Styrene (2.0 g, 19.2 mmol), alkoxyamine (5.0×10^{-5} mol) and toluene (1.8 ml) were added to a Pyrex ampoule, subjected to several freeze-degas-thaw cycles, and sealed under vacuum. Ampoules were heated at 110 °C for various times using an aluminium heating block. Reactions were quenched in an ice-water bath.

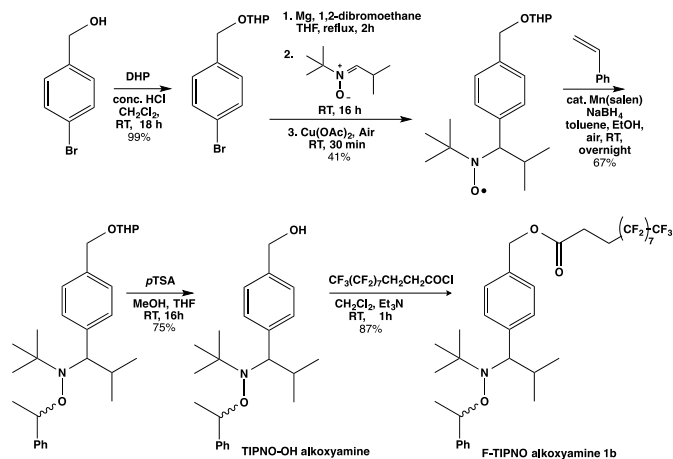
Precipitation polymerizations in supercritical carbon dioxide

The reactor (25 ml) was loaded with styrene (50% w/v loading, 12.5 g, 0.12 mol), alkoxyamine (3.125×10^{-4} mol) and a magnetic stirring bar and sealed. The reaction vessel was purged for 20 minutes by bubbling gaseous CO_2 through the reaction mixture. Liquid CO_2 (~5 MPa) was added and the reactor was immersed in an oil bath. The temperature was raised to the reaction temperature of 110 °C, followed by pressurizing the reaction vessel to 30 MPa by the addition of further CO_2 . Reactions were quenched by submersion of the reactor in an ice-water bath.

Results and discussion

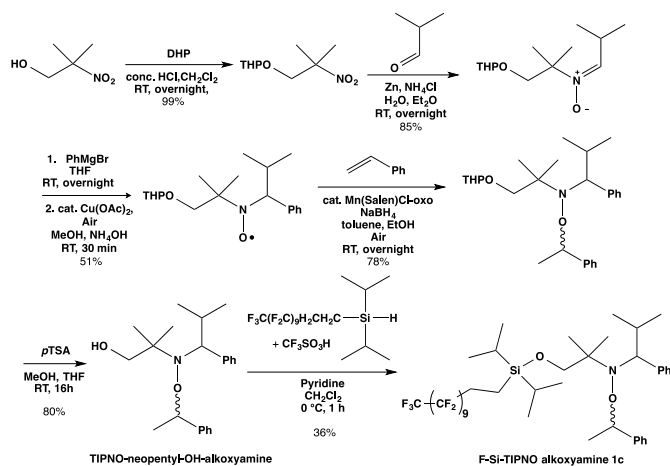
Synthesis of fluorinated alkoxyamine initiators

Three TIPNO-based alkoxyamine initiators were prepared for this study: F-TIPNO **1b** and F-Si-TIPNO **1c**, in which a fluorine fragment was attached to the nitroxide TIPNO, and TIPNO alkoxyamine F-Foot **2** in which the phenethyl “foot” of the alkoxyamine was labelled with a fluorine segment.



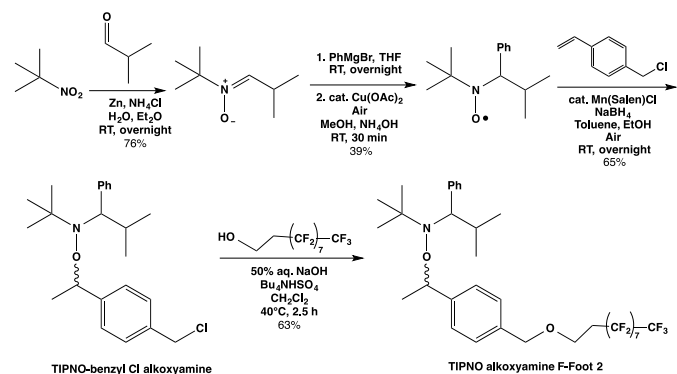
Scheme 3 Preparation of F-TIPNO alkoxyamine **1b**

For the preparation of F-TIPNO **1b** (Scheme 3), 4-bromobenzyl alcohol was protected using THP, and the Grignard reagent was prepared. The latter was a challenging reaction: the key to success was the use of 1,2-dibromoethane to enhance formation of the Grignard species. Following the standard TIPNO synthesis of addition to the nitrone and Cu-catalyzed oxidation to the nitroxide, treatment with styrene and Mn(salen) gave the THP-protected alkoxyamine. The synthetic technique required to make reliable Mn(salen) catalyst required careful air oxidation of the Mn-species while preparing the salen chloride complex, presumably forming the oxo species. Hot recrystallization, and discarding the orange portion of precipitate (the non-oxo species) gave a Mn(salen)Cl-oxo catalyst that was extremely effective in the styrene/nitroxide coupling reaction. Although the formation of this catalyst has been published previously,⁴⁵ this detailed experimental is included to ensure the repeatability of the alkoxyamine synthesis. Acid-mediated deprotection followed by esterification with the fluoralkane acid chloride provided F-TIPNO alkoxyamine **1b** bearing a tag containing 17 fluorine atoms.



Scheme 4 Preparation of F-Si-TIPNO alkoxyamine **1c**

F-Si-TIPNO **1c** was prepared starting with THP-protection of 2-methyl-2-nitropropan-1-ol (Scheme 4), followed by reductive condensation with isobutyryl aldehyde to give the THP protected nitrone. Addition of phenyl Grignard, oxidation and coupling with styrene using the Mn(salen) protocol afforded THP-protected alkoxyamine. Acidic removal of the protecting group, followed by silylation using the procedure of Crich⁴⁸ gave F-Si-TIPNO alkoxyamine **1c** bearing 21 fluorine atoms on the fluorous unit.



Scheme 5 Preparation of TIPNO alkoxyamine F-Foot **2**

The synthesis of the alkoxyamine containing a fluorous-tagged phenethyl “foot” portion proceeded by the normal synthesis of TIPNO,⁴³ coupling with styrene benzyl chloride, and etherification to provide TIPNO alkoxyamine F-Foot **2** (Scheme 5). This alkoxyamine contains a fluorous fragment consisting of a 17-fluorine atom segment on the portion of the initiator, which dissociates to become the first carbon radical of the polymerization sequence. Consequently, the fluorous tag is covalently attached to the growing polymer on the end distal to the nitroxide cap.

Solution polymerizations

TIPNO **1a** and TIPNO-derivative alkoxyamines **1b**, **1c** and alkoxyamine **2** all gave very similar rates of polymerization of styrene in toluene (50 % (w/v), Figure 1) at 110 °C, indicating that structural modifications to the nitroxide and styryl “foot” parts of the alkoxyamine have no significant effect on the equilibrium constant (*K*) for trapping and dissociation in organic solution.

As expected from the higher *K* for SG1,^{50, 51} the SG1-alkoxyamine **1d**-initiated polymerizations proceeded at a higher rate than TIPNO-derivatives **1a**, **1b**, **1c** and **2**. All alkoxyamine-initiated polymerizations in solution proceeded in a controlled/living manner with molecular weights close to theoretical values (eq. 1) and only less than theoretical values beyond about 55% conversion, although in most cases $M_w/M_n < 1.3$ throughout (Figure 2).

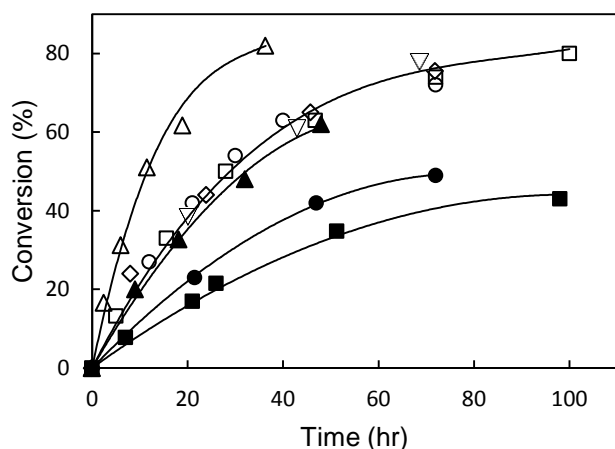


Figure 1 Conversion versus time plots for TIPNO-**1a** (circles), F-TIPNO-**1b** (squares), F-Si-TIPNO-**1c** (inverted triangle), SG1-**1d** (upright triangles) and TIPNO-F-Foot-**2** (diamonds), styryl-alkoxyamine initiated NMP of styrene (50% w/v) at 110 °C using $[\text{Monomer}]_0/[\text{Alkoxyamine}]_0 = 384$. Open and closed symbols are respectively solution in toluene and precipitation in scCO_2 at 30 MPa polymerizations.

Precipitation polymerizations in supercritical carbon dioxide (scCO_2)

For NMP of styrene (50% w/v) in scCO_2 at 110 °C and 30 MPa, the point of precipitation (J_{crit}) is predicted to occur at approximately $M_n = 3,450$ (~8.5% conv.) using the model developed by O'Connor et al,¹⁹ that can be used to estimate J_{crit} as a function of initial monomer loading and targeted molecular weight. Since NMPs in scCO_2 in the present article go beyond this conversion, all are considered heterogeneous systems. The alkoxyamine TIPNO **1a**-initiated styrene precipitation polymerization in scCO_2 proceeded at a similar rate to the analogous NMP carried out in the presence of a 5% excess of free TIPNO at lower conversions (23% conv. after 22 h as opposed to 19% conv. after 21 h, Figure 3), although the system containing an initial excess of free nitroxide reached a limiting conversion sooner (Figure S18a). Moreover, controlled/living character was good without the 5% excess of free TIPNO ($M_n = 7,960$ and $M_w/M_n = 1.22$), with the presence of excess free nitroxide providing a marginally narrower MWD ($M_n = 9,000$ and $M_w/M_n = 1.14$, also see Figure S18b for additional data showing the effect of free TIPNO on control/living character). It was therefore evident that controlled/living character for alkoxyamine-initiated precipitation polymerizations in scCO_2 can be established without the requirement for excess free nitroxide. Thus all subsequent NMPs in scCO_2 were initiated by alkoxyamines without the addition of free nitroxide. As previously observed by Aldabbagh et al.¹⁶ for bimolecular nitroxide/AIBN systems, polymerization rates are lower for precipitation polymerizations in scCO_2 in comparison to analogous solution polymerizations of styrene (Figure 1). This has been attributed to monomer partitioning, *i.e.* some styrene residing in the continuous scCO_2 phase after particle formation, leading to a lower

monomer concentration in the particles (the main locus of polymerization).

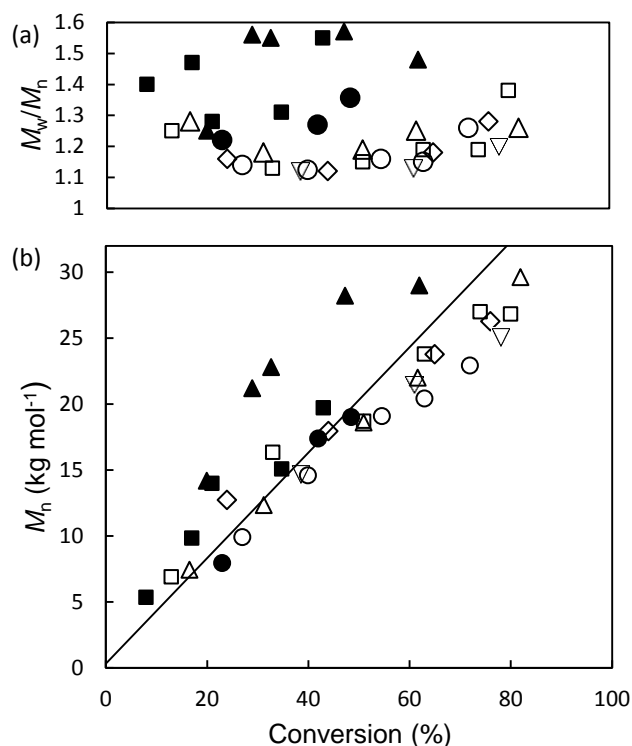


Figure 2 (a) Polydispersities (M_w/M_n) and (b) number-average molecular weights (M_n) versus conversion for TIPNO-**1a** (circles), F-TIPNO-**1b** (squares), F-Si-TIPNO-**1c** (inverted triangle), SG1-**1d** (upright triangles) and TIPNO-F-Foot-**2** (diamonds) styryl-alkoxyamine initiated NMP of styrene (50% w/v) at 110 °C using $[\text{Monomer}]_0/[\text{Alkoxyamine}]_0 = 384$. Open and closed symbols are respectively solution in toluene and precipitation in scCO_2 at 30 MPa polymerizations. The line represents theoretical MW ($M_{n,\text{theo}}$) based on Equation 1.

Very significant differences in polymerization rate and control are observed in scCO_2 between SG1-alkoxyamine **1d** and TIPNO-alkoxyamine **1a** with $M_n(\mathbf{1d}) > M_n(\mathbf{1a})$ and higher polydispersities for **1d** than **1a** (**1d**: $M_w/M_n = 1.25\text{-}1.57$ and **1a**: $M_w/M_n = 1.22\text{-}1.36$). The higher rate and inferior control for SG1 in scCO_2 is due to a combination of higher K_p ,^{50, 51} and a higher solubility of SG1 in scCO_2 , leading to greater nitroxide partitioning away from the locus of polymerization after particle formation. Although there is no literature data available for nitroxide solubilities in scCO_2 , one may expect a greater solubility for TIPNO in the organic phase (particles) due to TIPNO's organic nature in comparison to SG1, which contains heteroatoms (e.g. phosphorous). Poor control for SG1-mediated polymerizations in scCO_2 were not previously observed in bimolecular nitroxide/AIBN systems in scCO_2 because of the use of a high ratio of $[\text{SG1}]_0/[\text{AIBN}]_0$.^{13, 15-17} Despite TIPNO **1a** and fluorinated alkoxyamine F-TIPNO **1b**-initiated NMP exhibiting the same rate of polymerization in solution, unexpectedly the **1a**-initiated NMP was marginally faster in scCO_2 . The fluorinated nitroxide **1b** is more CO_2 -philic than TIPNO **1a**, and is expected to

partition away from the locus of polymerization upon particle formation, which should lead to a higher rate rather than the observed lower rate of polymerization for **1b**.

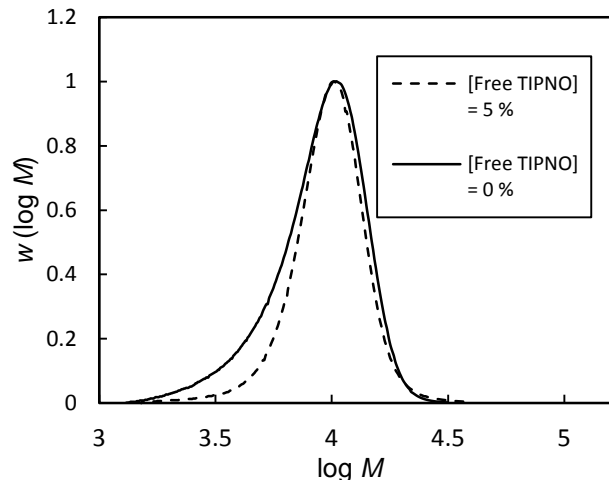


Figure 3 Effect of free nitroxide on MWDs for the precipitation NMP of 50% (w/v) styrene at 30 MPa and 110 °C using $[\text{Monomer}]_0/[\text{Alkoxyamine}]_0 = 384$. $[\text{Free TIPNO}]_0/[\text{Alkoxyamine } \mathbf{1a}]_0 = 0.05$, dashed line is 19% conv. after 21 h, $M_n = 9,000$ and $M_w/M_n = 1.14$ and the solid line is 23% conv. after 22 h, $M_n = 7,960$ and $M_w/M_n = 1.22$.

To understand the effects of nitroxide partitioning more quantitatively, modelling and simulations were conducted using PREDICI⁵² for the St/TIPNO system at 110 °C using a previously published approach⁵³ (the model used here was identical, with the exception of the inclusion in this work of a reaction step for spontaneous (thermal) initiation of styrene according to: $R_{i,th} = k_{i,th}[\text{St}]^3$). Conditions and parameters: $[\text{St}]_0 = 8.7 \text{ M}$, $[\text{alkoxyamine}]_0 = 0.0227 \text{ M}$, propagation rate coeff. $(k_p)^{54} = 1580 \text{ M}^{-1}\text{s}^{-1}$, termination rate coeff. $(k_t)^{55} = 1.57 \times 10^8 \text{ M}^{-1}\text{s}^{-1}$ (combination only), activation rate coeff. $(k_{act})^{50} = 1.184 \times 10^{-3} \text{ s}^{-1}$, deactivation rate coeff. $(k_{deact})^{51} = 8.2 \times 10^6 \text{ M}^{-1}\text{s}^{-1}$, thermal initiation of styrene $(k_{i,th})^{56} = 4.26 \times 10^{-11} \text{ M}^{-1}\text{s}^{-1}$. The system modelled is a bulk polymerization with a fictitious nitroxide partitioning step into a continuous phase (*i.e.* the scCO₂ phase) having the same volume as the organic phase, whereby a given fraction of free nitroxide is removed (equivalent to partitioning to the continuous phase) assuming phase transfer equilibrium. Figures 4 and 5 show conversion vs time data and MWDs obtained for different partition coefficients of $\Gamma = [\text{nitroxide}]_{org}/[\text{nitroxide}]_{CO_2} = \infty$ (no partitioning), 1 and 0.25. $\Gamma = 1$ and 0.25 correspond to situations where 50% and 80% of free nitroxide, respectively, is located in the continuous phase. It is apparent that even if very extensive nitroxide partitioning occurs, the increase in rate of polymerization is relatively small. Figure 5 shows that as expected, there is a broadening of the MWDs with increasing nitroxide partitioning, with the livingness (number fraction of chains with alkoxyamine-terminated α -ends at 48% conversion) decreasing according to 97.5, 96.8, 95.3% with increasing partitioning. Indeed the alkoxyamine-initiated polymerizations using fluorinated TIPNO derivative **1b** ($M_w/M_n = 1.25$ -1.55) proceeded with inferior control

relative to TIPNO **1a**, as demonstrated by M_n s higher than theoretical values and higher polydispersities (Figures 2).

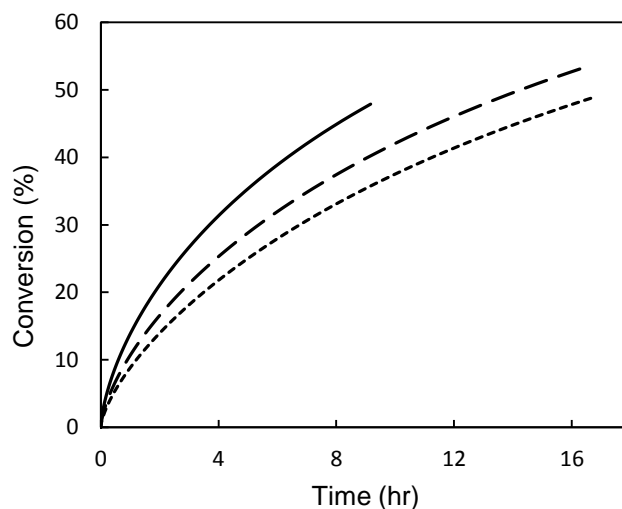


Figure 4 Simulated conversion vs time data of the styrene/TIPNO system at 110 °C (see text for details). $[\text{nitroxide}]_{org}/[\text{nitroxide}]_{CO_2} = \infty$ (dotted line), 1 (dashed line), and 0.25 (solid line). $\Gamma = \infty$, 1 and 0.25 correspond to situations where 0, 50 and 80% of free nitroxide, respectively, is located in the continuous phase.

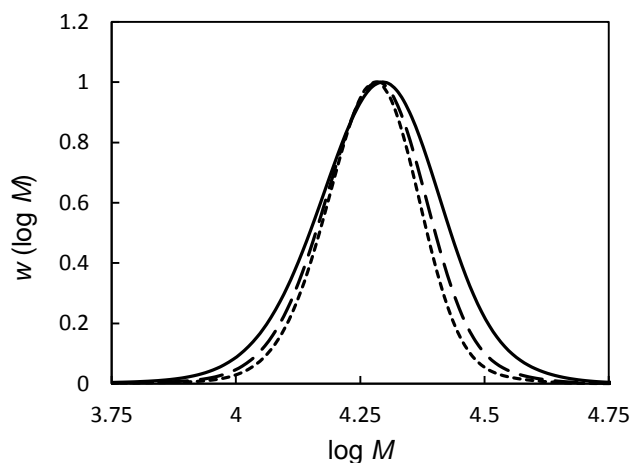


Figure 5 Simulated MWDs (at 48% conv.) of the styrene/TIPNO system at 110 °C. $[\text{nitroxide}]_{org}/[\text{nitroxide}]_{CO_2} = \infty$ (dotted line), 1 (dashed line), and 0.25 (solid line). $\Gamma = \infty$, 1 and 0.25 correspond to situations where 0, 50 and 80% of free nitroxide, respectively, is located in the continuous phase.

If nitroxide partitioning is the main cause of inferior control for alkoxyamine **1b** in scCO₂, it follows that the polymerization rate is quite insensitive to the degree of nitroxide partitioning, more so than one would have expected. As such it may be reasonable to argue that the relatively small difference in the rate of polymerization between TIPNO **1a** and F-TIPNO **1b** in scCO₂ is not necessarily inconsistent with F-TIPNO nitroxide partitioning away from the locus of polymerization resulting in wider MWDs.

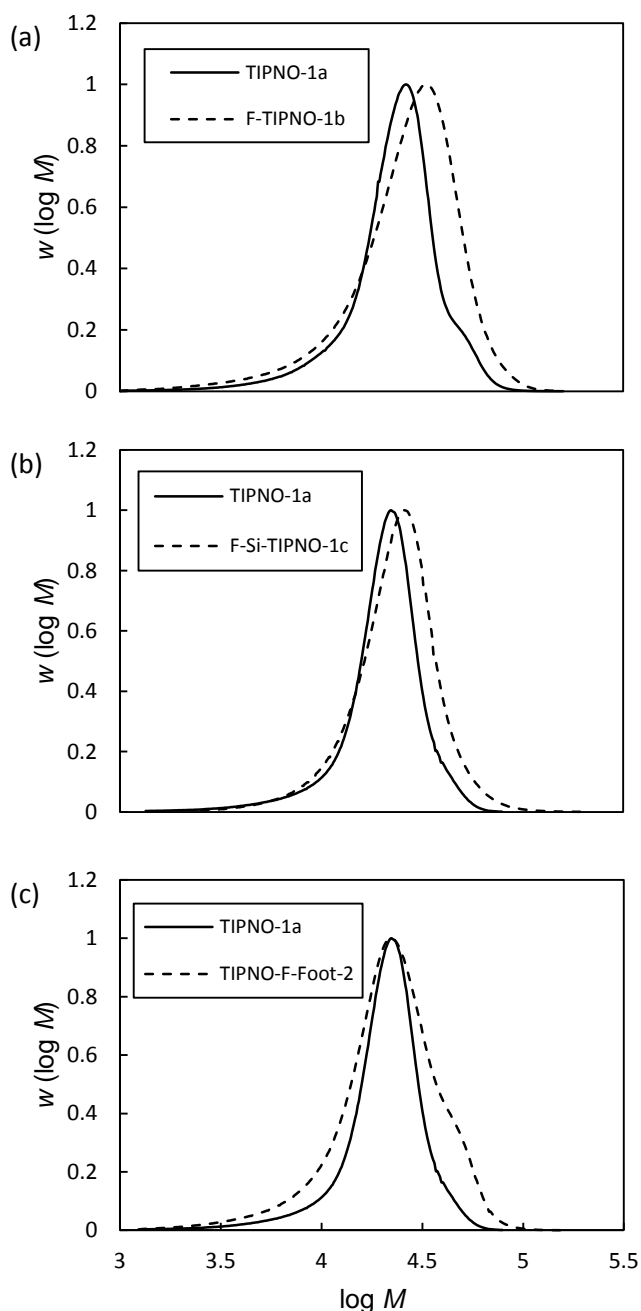


Figure 6 Comparing the performance of fluorinated alkoxyamines **1b**, **1c** and **2** with the TIPNO analogue **1a** in the precipitation NMP of styrene (50% w/v) at 110 °C using $[\text{Monomer}]_0/[\text{Alkoxyamine}]_0 = 384$. (a) TIPNO-**1b**, 43% after 98 h, $M_n = 19,700$ and $M_w/M_n = 1.55$ compared with TIPNO-**1a** initiated analogue, 49% after 72 h, $M_n = 19,000$ and $M_w/M_n = 1.36$ (b) TIPNO-**1c**, 39% conv. after 61 h, $M_n = 20,000$ and $M_w/M_n = 1.29$ compared with the TIPNO-**1a** initiated analogue, 42% conv. after 47 h, $M_n = 17,400$ and $M_w/M_n = 1.27$ (c) TIPNO-F-Foot-**2**, 38% conv. after 69 h, $M_n = 19,500$ and $M_w/M_n = 1.32$ compared with the TIPNO-**1a** initiated analogue, 42% conv. after 47 h, $M_n = 17,400$ and $M_w/M_n = 1.27$.

Moreover similar to the simulated MWD overlays in Figure 5, nitroxide partitioning seems to give marginal broadening experimentally (Figure 6a), when comparing MWDs for TIPNO **1a** with the F-TIPNO **1b**-initiated polymerization at similar intermediate conversions.

Precipitation polymerizations of styrene in scCO_2 for fluorinated alkoxyamines F-Si-TIPNO **1c** and TIPNO alkoxyamine F-foot **2** were carried out (Figures 6b and 6c). Broadening for **1c** was analogous to F-TIPNO **1b**-initiated polymerization in scCO_2 with the alkoxyamine **2** experiment also giving a high MW shoulder, in the case of **1c** presumably due to nitroxide partitioning as discussed above for **1b**. Again, contrary to expectation, the polymerization rate for **1c** was somewhat lower than for **1a**. Alkoxyamine **2** differs from the other fluorinated alkoxyamines **1b** and **1c** in that (non-fluorinated) TIPNO is the mediating nitroxide and a fluorinated initiating styryl “foot” radical is produced upon dissociation. As such, the extent of nitroxide partitioning would be expected to be the same as for **1a**. One can speculate that the F-content in the propagating radical part of the alkoxyamine leads to an increase in J_{crit} (due to increased solubility in the continuous phase), and thus later nucleation; it is possible that this is related to the partial loss of control. It is unlikely that a higher k_d for TIPNO-F-foot **2** is causing the observed MWD broadening in comparison to TIPNO-**1a** alkoxyamine, because rates and control are very similar in solution (toluene), assuming negligible solvent effects on activation-deactivation kinetics in scCO_2 .

Conclusions

In the absence of excess free $[\text{nitroxide}]_0$, TIPNO alkoxyamine is found to give superior controlled/living character for precipitation NMP of styrene in scCO_2 compared to the SG1 analogue. In solution (toluene), the latter system resulted in slightly less control and a higher rate of polymerization. Differences between TIPNO- and SG1-alkoxyamine can be rationalised in terms of the higher K for SG1 and a greater level of nitroxide partitioning for SG1 in the heterogeneous system. Despite increased steric congestion about the alkoxyamine (N-O bond) in novel fluorinated TIPNO-alkoxyamine initiators, a similar equilibrium constant (K) to TIPNO for activation/deactivation in organic solution can be inferred. The greater partitioning of fluorinated TIPNO derivatives in scCO_2 impacts on the controlled/living character, broadening the molecular weight distributions.

Acknowledgements

This work received financial support as part of the first IUPAC Transnational Call in Polymer Chemistry funded by awards from the Irish Research Council (formerly IRCSET) to F. Aldabbagh and the National Science Foundation (NSF CHE-1057927, USA) to R. Braslau.

Notes and References

1. J. L. Kendall, D. A. Canelas, J. L. Young and J. M. DeSimone, *Chem. Rev.*, 1999, **99**, 543-563.
2. P. B. Zetterlund, F. Aldabbagh and M. Okubo, *J. Polym. Sci., Part A: Polym. Chem.*, 2009, **47**, 3711-3728.
3. K. J. Thurecht and S. M. Howdle, *Aust. J. Chem.*, 2009, **62**, 786-789.
4. R. Span and W. Wagner, *J. Phys. Chem. Ref. Data*, 1996, **25**, 1509-1596.
5. F. Rindfleisch, T. P. DiNoia and M. A. McHugh, *J. Phys. Chem.*, 1996, **100**, 15581-15587.
6. Y. Sugihara, P. O'Connor, P. B. Zetterlund and F. Aldabbagh, *J. Polym. Sci., Part A: Polym. Chem.*, 2011, **49**, 1856-1864.
7. C. Magee, Y. Sugihara, P. B. Zetterlund and F. Aldabbagh, *Polym. Chem.*, 2014, **5**, 2259-2265.
8. P. O'Connor, P. B. Zetterlund and F. Aldabbagh, *J. Polym. Sci., Part A: Polym. Chem.*, 2011, **49**, 1719-1723.
9. P. O'Connor, R. Yang, W. M. Carroll, Y. Rochev and F. Aldabbagh, *Eur. Polym. J.*, 2012, **48**, 1279-1288.
10. J. Nicolas, Y. Guillaneuf, C. Lefay, D. Bertin, D. Gimes and B. Charleux, *Prog. Polym. Sci.*, 2013, **38**, 63-235.
11. P. G. Odell and G. K. Hamer, *Polym. Mater. Sci. Eng.*, 1996, **74**, 404-405.
12. J. Ryan, F. Aldabbagh, P. B. Zetterlund and M. Okubo, *Polymer*, 2005, **46**, 9769-9777.
13. R. McHale, F. Aldabbagh, P. B. Zetterlund, H. Minami and M. Okubo, *Macromolecules*, 2006, **39**, 6853-6860.
14. R. McHale, F. Aldabbagh, P. B. Zetterlund and M. Okubo, *Macromol. Rapid Commun.*, 2006, **27**, 1465-1471.
15. R. McHale, F. Aldabbagh, P. B. Zetterlund and M. Okubo, *Macromol. Chem. Phys.*, 2007, **208**, 1813-1822.
16. F. Aldabbagh, P. B. Zetterlund and M. Okubo, *Eur. Polym. J.*, 2008, **44**, 4037-4046.
17. F. Aldabbagh, P. B. Zetterlund and M. Okubo, *Macromolecules*, 2008, **41**, 2732-2734.
18. D. G. Ramirez-Wong, C. A. Posada-Velez, E. Saldivar-Guerra, J. G. Luna-Barcenas, C. Ott and U. S. Schubert, *Macromol. Symp.*, 2009, **283-284**, 120-129.
19. P. O'Connor, P. B. Zetterlund and F. Aldabbagh, *Macromolecules*, 2010, **43**, 914-919.
20. B. Grignard, T. Phan, D. Bertin, D. Gimes, C. Jerome and C. Detrembleur, *Polymer Chemistry*, 2010, **1**, 837-840.
21. O. Garcia-Valdez, D. G. Ramirez-Wong, E. Saldivar-Guerra and G. Luna-Barcenas, *Macromol. Chem. Phys.*, 2013, **214**, 1396-1404.
22. K. Matyjaszewski, *Macromolecules*, 2012, **45**, 4015-4039.
23. J. Xia, T. Johnson, S. G. Gaynor, K. Matyjaszewski and J. DeSimone, *Macromolecules*, 1999, **32**, 4802-4805.
24. H. Minami, Y. Kagawa, S. Kuwahara, J. Shigematsu, S. Fujii and M. Okubo, *Des. Monomers Polym.*, 2004, **7**, 553-562.
25. B. Grignard, C. Jerome, C. Calberg, R. Jerome and C. Detrembleur, *Eur. Polym. J.*, 2008, **44**, 861-871.
26. B. Grignard, C. Jerome, C. Calberg, R. Jerome, W. Wang, S. M. Howdle and C. Detrembleur, *Chem. Commun.*, 2008, 314-316.
27. B. Grignard, C. Jerome, C. Calberg, R. Jerome, W. Wang, S. M. Howdle and C. Detrembleur, *Macromolecules*, 2008, **41**, 8575-8583.
28. B. Grignard, C. Calberg, C. Jerome and C. Detrembleur, *J. Supercrit. Fluids*, 2010, **53**, 151-155.
29. H. Minami, A. Tanaka, Y. Kagawa and M. Okubo, *J. Polym. Sci., Part A: Polym. Chem.*, 2012, **50**, 2578-2584.
30. G. Moad, E. Rizzardo and S. H. Thang, *Aust. J. Chem.*, 2012, **65**, 985-1076.
31. K. J. Thurecht, A. M. Gregory, W. Wang and S. M. Howdle, *Macromolecules*, 2007, **40**, 2965-2967.
32. A. M. Gregory, K. J. Thurecht and S. M. Howdle, *Macromolecules*, 2008, **41**, 1215-1222.
33. H. Lee, E. Terry, M. Zong, N. Arrowsmith, S. Perrier, K. J. Thurecht and S. M. Howdle, *J. Am. Chem. Soc.*, 2008, **130**, 12242-12243.
34. M. Zong, K. J. Thurecht and S. M. Howdle, *Chem. Commun.*, 2008, 5942-5944.
35. G. Jaramillo-Soto, P. R. Garcia-Moran, F. J. Enriquez-Medrano, H. Maldonado-Textle, M. E. Albores-Velasco, R. Guerrero-Santos and E. Vivaldo-Lima, *Polymer*, 2009, **50**, 5024-5030.
36. J. Jennings, M. Beija, A. P. Richez, S. D. Cooper, P. E. Mignot, K. J. Thurecht, K. S. Jack and S. M. Howdle, *J. Am. Chem. Soc.*, 2012, **134**, 4772-4781.
37. G. Jaramillo-Soto and E. Vivaldo-Lima, *Aust. J. Chem.*, 2012, **65**, 1177-1185.
38. G. Jaramillo-Soto, C. M. Villa-Avila and E. Vivaldo-Lima, *J. Macromol. Sci., Part A: Pure Appl. Chem.*, 2013, **50**, 281-286.
39. J. Jennings, M. Beija, J. T. Kennon, H. Willcock, R. K. O'Reilly, S. Rimmer and S. M. Howdle, *Macromolecules*, 2013, **46**, 6843-6851.
40. T. Taniyama, T. Kuroda, H. Minami and M. Okubo, *Polym. J.*, 2012, **44**, 1082-1086.
41. T. Kuroda, A. Tanaka, T. Taniyama, H. Minami, A. Goto, T. Fukuda and M. Okubo, *Polymer*, 2012, **53**, 1212-1218.
42. J. Dao, D. Benoit and C. J. Hawker, *J. Polym. Sci., Part A: Polym. Chem.*, 1998, **36**, 2161-2167.
43. D. Benoit, V. Chaplinski, R. Braslau and C. J. Hawker, *J. Am. Chem. Soc.*, 1999, **121**, 3904-3920.
44. R. Cuervo-Rodriguez, V. Bordege, M. C. Fernandez-Monreal, M. Fernandez-Garcia and E. L. Madruga, *J. Polym. Sci., Part A: Polym. Chem.*, 2004, **42**, 4168-4176.
45. M. Bothe and G. Schmidt-Naake, *Macromol. Rapid Commun.*, 2003, **24**, 609-613.
46. M. Rodlert, E. Harth, I. Rees and C. J. Hawker, *J. Polym. Sci., Part A: Polym. Chem.*, 2000, **38**, 4749-4763.
47. J. Ruehl and R. Braslau, *J. Polym. Sci., Part A: Polym. Chem.*, 2007, **45**, 2015-2025.
48. D. Crich, D. Grant and A. A. Bowers, *J. Am. Chem. Soc.*, 2007, **129**, 12106-12107.
49. L. Valtola, A. Koponen, M. Karesoja, S. Hietala, A. Laukkanen, H. Tenhu and P. Denifl, *Polymer*, 2009, **50**, 3103-3110.

50. S. Marque, M. C. Le, P. Tordo and H. Fischer, *Macromolecules*, 2000, **33**, 4403-4410.
51. J. Sobek, R. Martschke and H. Fischer, *J. Am. Chem. Soc.*, 2001, **123**, 2849-2857.
52. M. Wulkow, *Macromol. React. Eng.*, 2008, **2**, 461-494.
53. P. B. Zetterlund, *Macromol. Theory Simul.*, 2010, **19**, 11-23.
54. M. Buback, R. G. Gilbert, R. A. Hutchinson, B. Klumperman, F.-D. Kuchta, B. G. Manders, K. F. O'Driscoll, G. T. Russell and J. Schweer, *Macromol. Chem. Phys.*, 1995, **196**, 3267-3280.
55. M. Buback, C. Kowollik, C. Kurz and A. Wahl, *Macromol. Chem. Phys.*, 2000, **201**, 464-469.
56. A. W. Hui and A. E. Hamielec, *J. Appl. Polym. Sci.*, 1972, **16**, 749-769.